

UC Berkeley

Archaeological X-ray Fluorescence Reports

Title

SOURCE PROVENANCE OF OBSIDIAN ARTIFACTS FROM A BASKETMAKER III SITE IN CHACO CANYON NATIONAL HISTORIC PARK, NORTHWEST NEW MEXICO

Permalink

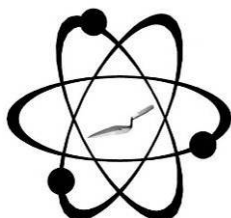
<https://escholarship.org/uc/item/51m9x1s9>

Author

Shackley, M. Steven

Publication Date

2017-08-10

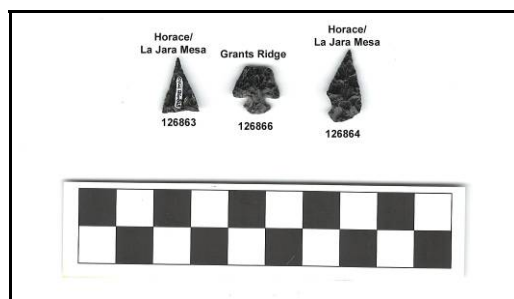


GEOARCHAEOLOGICAL XRF LAB
A GREEN SOLAR FACILITY

GEOARCHAEOLOGICAL X-RAY FLUORESCENCE SPECTROMETRY LABORATORY
8100 WYOMING BLVD., SUITE M4-158

ALBUQUERQUE, NM 87113 USA

**SOURCE PROVENANCE OF OBSIDIAN ARTIFACTS FROM A BASKETMAKER III SITE IN
CHACO CANYON NATIONAL HISTORIC PARK, NORTHWEST NEW MEXICO**



Three projectile point fragments from the site, all produced from Mount Taylor sources, as is much of the debitage in the site
(to approximate scale)

by

M. Steven Shackley Ph.D., Director
Geoarchaeological XRF Laboratory
Albuquerque, New Mexico

Report Prepared for

Chaco Culture National Historic Park
Nageezi, New Mexico

14 August 2017

INTRODUCTION

The analysis here of 63 artifacts from a BMIII site at Chaco Culture National History Park, northwest New Mexico indicates a diverse obsidian provenance assemblage dominated by northern New Mexico Jemez Lineament obsidian sources, particularly those in the southern Jemez Mountains (Canovas Canyon Rhyolite - 48.3%, and the two sources in the Mount Taylor Volcanic Field (Horace/La Jara Mesa - 31.7%, and Grants Ridge - 10%). A few of the artifacts were produced from three other Jemez Mountains sources (Valles Rhyolite-Cerro del Medio, n=4; and Cerro Toledo Rhyolite and El Rechuelos, one each). Based on the obsidian source provenance, the results suggest a relatively large procurement range/interaction sphere, and habitation of this site possibly after movement from the south and/or east (see discussion).

LABORATORY SAMPLING, ANALYSIS AND INSTRUMENTATION

All archaeological samples are analyzed whole. The results presented here are quantitative in that they are derived from "filtered" intensity values ratioed to the appropriate x-ray continuum regions through a least squares fitting formula rather than plotting the proportions of the net intensities in a ternary system (McCarthy and Schamber 1981; Schamber 1977). Or more essentially, these data through the analysis of international rock standards, allow for inter-instrument comparison with a predictable degree of certainty (Hampel 1984; Shackley 2011).

All analyses for this study were conducted on a ThermoScientific *Quant'X* EDXRF spectrometer, located in the Geoarchaeological XRF Laboratory, Albuquerque, New Mexico. It is equipped with a thermoelectrically Peltier cooled solid-state Si(Li) X-ray detector, with a 50 kV, 50 W, ultra-high-flux end window bremsstrahlung, Rh target X-ray tube and a 76 μm (3 mil) beryllium (Be) window (air cooled), that runs on a power supply operating 4-50 kV/0.02-1.0 mA at 0.02 increments. The spectrometer is equipped with a 200 l min^{-1} Edwards vacuum pump, allowing for the analysis of lower-atomic-weight elements between sodium (Na) and titanium

(Ti). Data acquisition is accomplished with a pulse processor and an analogue-to-digital converter. Elemental composition is identified with digital filter background removal, least squares empirical peak deconvolution, gross peak intensities and net peak intensities above background.

For the analysis of mid Zb condition elements Ti-Nb, Pb, Th, the x-ray tube is operated at 30 kV, using a 0.05 mm (medium) Pd primary beam filter in an air path at 100 or 200 seconds livetime, depending on artifact size (Davis et al. 2011) to generate x-ray intensity $K\alpha$ -line data for elements titanium (Ti), manganese (Mn), iron (as $Fe_2O_3^T$), cobalt (Co), nickel (Ni), copper, (Cu), zinc, (Zn), gallium (Ga), rubidium (Rb), strontium (Sr), yttrium (Y), zirconium (Zr), niobium (Nb), lead (Pb), and thorium (Th). Not all these elements are reported since their values in many volcanic rocks are very low. Trace element intensities were converted to concentration estimates by employing a least-squares calibration line ratioed to the Compton scatter established for each element from the analysis of international rock standards certified by the National Institute of Standards and Technology (NIST), the US. Geological Survey (USGS), Canadian Centre for Mineral and Energy Technology, and the Centre de Recherches Pétrographiques et Géochimiques in France (Govindaraju 1994). Line fitting is linear (XML) for all elements. When barium (Ba) is acquired in the High Zb condition, the Rh tube is operated at 50 kV and up to 1.0 mA, ratioed to the bremsstrahlung region (see Davis 2011; Shackley 2011). Further details concerning the petrological choice of these elements in Southwest obsidians is available in Shackley (1988, 1995, 2005; also Mahood and Stimac 1991; and Hughes and Smith 1993). Nineteen specific pressed powder standards are used for the best fit regression calibration for elements Ti-Nb, Pb, Th, and Ba, include G-2 (basalt), AGV-2 (andesite), GSP-2 (granodiorite), SY-2 (syenite), BHVO-2 (hawaiite), STM-1 (syenite), QLO-1 (quartz latite), RGM-1 (obsidian), W-2 (diabase), BIR-1 (basalt), SDC-1 (mica schist), TLM-1 (tonalite), SCO-1 (shale), NOD-A-1

and NOD-P-1 (manganese) all US Geological Survey standards, NIST-278 (obsidian), U.S. National Institute of Standards and Technology, BE-N (basalt) from the Centre de Recherches Pétrographiques et Géochimiques in France, and JR-1 and JR-2 (obsidian) from the Geological Survey of Japan (Govindaraju 1994).

The data from the WinTrace™ software were translated directly into Excel for Windows for manipulation and on into SPSS™ 21.0 for Windows and JMP™ 4.0.1 for Windows for statistical analyses. In order to evaluate these quantitative determinations, machine data were compared to measurements of known standards during each run. RGM-1 a USGS obsidian standard is analyzed during each sample run for obsidian artifacts to check machine calibration (Table 1). Source assignments were made with reference to Shackley (1995, 1998, 2005, 2009), Shackley et al. (2016) and source standard data at this lab (Table 1, and Figures 1 and 2). Many of the samples were near or below the minimum size to insure confident source assignment (Davis et al. 2011). Longer counts and acquisition of Ba was used to mitigate this issue (see Davis et al. 2011; Shackley2011).

DISCUSSION

As noted above, all of the artifacts were produced from obsidian sources well to the south and east of Chaco Canyon, dominated by Canovas Canyon Rhyolite, also called Bear Springs Peak (over 125 linear km east), and the two sources in the Mount Taylor Volcanic Field (about 100 km south; Tables 1 and 2, and Figures 3 and 4). This is a minimum procurement range for these Basketmaker III knappers that is over a 125 linear km radius east and south, not unusual in Archaic/Basketmaker periods (Shackley 1989, 1996, 2005).

The dominance of Canovas Canyon Rhyolite is unusual in my experience in this time period in the region, even in sites nearer the source (Shackley 2014, 2015; Shackley et al. 2016). Another Keres Member source in the southern Jemez Mountains, Bearhead Rhyolite, also called

Paliza Canyon, that is numerically superior at the source, is absent in the assemblage even though it is located in the same area (Shackley et al. 2016). This could mean that the Canovas Canyon raw material was collected in secondary deposits along Vallecito Creek south of the primary source around Bear Spring Peak, and potentially on the way to or from Mount Taylor, or simply part of the procurement range, or interaction sphere (see Figure 4). To be fair, these are the nearest sources to Chaco Canyon, but there seems to be some raw material selection, particularly given the dominance of Canovas Canyon Rhyolite versus the numerically superior Bearhead Rhyolite (similar flaking properties and more nodules and larger nodule sizes).

Regardless of what agency was used to get raw material to the site (direct procurement or exchange) the technology dominated by biface thinning flakes, and an absence of cores suggests projectile point maintenance and rejuvenation. The three projectile points were produced from the Mount Taylor sources that comprises about 42% of the obsidian assemblage (see cover image). Other projectile points and cores could have been present in a portion of the site not excavated, or more likely primary reduction occurred at the source or on the way from these source areas. If correct, this would be an argument for direct procurement and the obsidian source provenance as a reflection of procurement range (see Shackley 1996, 2005).

REFERENCES CITED

- Davis, K.D., T.L. Jackson, M.S. Shackley, T. Teague, and J.H. Hampel
2011 Factors Affecting the Energy-Dispersive X-Ray Fluorescence (EDXRF) Analysis of Archaeological Obsidian. In *X-Ray Fluorescence Spectrometry (XRF) in Geoarchaeology*, edited by M.S. Shackley, pp. 45-64. Springer, New York.
- Govindaraju, K.
1994 1994 Compilation of Working Values and Sample Description for 383 Geostandards. *Geostandards Newsletter* 18 (special issue).
- Hampel, Joachim H.
1984 Technical Considerations in X-ray Fluorescence Analysis of Obsidian. In *Obsidian Studies in the Great Basin*, edited by R.E. Hughes, pp. 21-25. Contributions of the University of California Archaeological Research Facility 45. Berkeley.

Hildreth, W.

1981 Gradients in Silicic Magma Chambers: Implications for Lithospheric Magmatism. *Journal of Geophysical Research* 86:10153-10192.

Hughes, Richard E., and Robert L. Smith

1993 Archaeology, Geology, and Geochemistry in Obsidian Provenance Studies. In *Scale on Archaeological and Geoscientific Perspectives*, edited by J.K. Stein and A.R. Linse, pp. 79-91. Geological Society of America Special Paper 283.

Mahood, Gail A., and James A. Stimpac

1990 Trace-Element Partitioning in Pantellerites and Trachytes. *Geochemica et Cosmochimica Acta* 54:2257- 2276.

McCarthy, J.J., and F.H. Schamber

1981 Least-Squares Fit with Digital Filter: A Status Report. In *Energy Dispersive X-ray Spectrometry*, edited by K.F.J. Heinrich, D.E. Newbury, R.L. Myklebust, and C.E. Fiori, pp. 273-296. National Bureau of Standards Special Publication 604, Washington, D.C.

Schamber, F.H.

1977 A Modification of the Linear Least-Squares Fitting Method which Provides Continuum Suppression. In *X-ray Fluorescence Analysis of Environmental Samples*, edited by T.G. Dzubay, pp. 241-257. Ann Arbor Science Publishers.

Shackley, M. Steven

1988 Sources of Archaeological Obsidian in the Southwest: An Archaeological, Petrological, and Geochemical Study. *American Antiquity* 53(4):752-772.

1989 *Early Hunter-Gatherer Procurement Ranges in the Southwest: Evidence from Obsidian Geochemistry and Lithic Technology*. Ph.D. dissertation, Department of Anthropology, Arizona State University, Tempe.

1995 Sources of Archaeological Obsidian in the Greater American Southwest: An Update and Quantitative Analysis. *American Antiquity* 60(3):531-551.

1996 Range and Mobility in the Early Hunter-Gatherer Southwest. In *Early Formative Adaptations in the Southern Southwest*, edited by Barbara Roth, pp. 5-16. Monographs in World Prehistory 25. Prehistory Press, Madison.

1998 Geochemical Differentiation and Prehistoric Procurement of Obsidian in the Mount Taylor Volcanic Field, Northwest New Mexico. *Journal of Archaeological Science* 25:1073-1082.

2005 *Obsidian: Geology and Archaeology in the North American Southwest*. University of Arizona Press, Tucson.

2009 Two Newly Discovered Sources of Archaeological Obsidian in the Southwest: Archaeological and Social Implications. *Kiva* 74:269-280.

2011 An Introduction to X-Ray Fluorescence (XRF) Analysis in Archaeology. In *X-Ray Fluorescence Spectrometry (XRF) in Geoarchaeology*, edited by M.S. Shackley, pp. 7-44. Springer, New York.

2014 Source provenance of obsidian artifacts from 17 archaeological sites along the MAPL WEPIII project alignment, northwestern to southeastern New Mexico: unpublished report prepared for the Office of Contract Archeology, University of New Mexico, Albuquerque.

2015 Source provenance of obsidian artifacts from The El Segundo archaeology project, Northwestern New Mexico: unpublished report prepared for Southwest Archaeological Consultants, Santa Fe, New Mexico

Shackley, M.S., F. Goff, and S.G. Dolan

2016 Geologic Origin of the Source of Bearhead Rhyolite (Paliza Canyon) Obsidian, Jemez Mountains, Northern New Mexico. *New Mexico Geology* 38:52-62.

Table 1. Elemental concentrations and source assignments for the archaeological specimens, and analysis of USGS RGM-1 obsidian standard. All measurements in parts per million (ppm).

| Sample | Mn | Zn | Rb | Sr | Y | Zr | Nb | Ba ¹ | Source |
|----------|-----|-----|-----|----|----|-----|-----|-----------------|-------------------------------|
| 126863 | 603 | 266 | 529 | 14 | 95 | 131 | 217 | | Horace/La Jara Mesa-Mt Taylor |
| 126864 | 629 | 244 | 552 | 15 | 94 | 143 | 224 | | Horace/La Jara Mesa-Mt Taylor |
| 126866 | 791 | 225 | 572 | 11 | 80 | 121 | 187 | | Grants Ridge-Mt Taylor |
| 126877 | 576 | 242 | 548 | 10 | 89 | 140 | 222 | | Horace/La Jara Mesa-Mt Taylor |
| 126880 | 550 | 190 | 487 | 16 | 87 | 132 | 220 | | Horace/La Jara Mesa-Mt Taylor |
| 126887 | 533 | 391 | 105 | 40 | 17 | 78 | 38 | 80 | Canovas Canyon Rhy |
| 126888 | 437 | 122 | 118 | 44 | 23 | 98 | 53 | 397 | Canovas Canyon Rhy |
| 126898 | 852 | 232 | 606 | 16 | 83 | 112 | 187 | | Grants Ridge-Mt Taylor |
| 126882-1 | 411 | 87 | 115 | 48 | 22 | 98 | 51 | | Canovas Canyon Rhy |
| 126882-2 | 672 | 273 | 557 | 13 | 99 | 139 | 231 | | Horace/La Jara Mesa-Mt Taylor |
| 126882-3 | 590 | 268 | 518 | 14 | 90 | 135 | 217 | | Horace/La Jara Mesa-Mt Taylor |
| 126885 | 719 | 337 | 588 | 17 | 96 | 142 | 218 | | Horace/La Jara Mesa-Mt Taylor |
| 126895-1 | 620 | 274 | 554 | 12 | 95 | 141 | 217 | | Horace/La Jara Mesa-Mt Taylor |
| 126895-2 | 550 | 141 | 136 | 48 | 18 | 101 | 47 | | Canovas Canyon Rhy |
| 126900 | 453 | 296 | 115 | 44 | 19 | 88 | 41 | 348 | Canovas Canyon Rhy |
| 126901-1 | 636 | 492 | 506 | 13 | 80 | 115 | 175 | | Grants Ridge-Mt Taylor |
| 126901-2 | 594 | 224 | 539 | 11 | 90 | 145 | 221 | | Horace/La Jara Mesa-Mt Taylor |
| 126901-3 | 765 | 320 | 595 | 13 | 89 | 143 | 228 | | Horace/La Jara Mesa-Mt Taylor |
| 126901-4 | 835 | 391 | 618 | 13 | 85 | 144 | 209 | | Horace/La Jara Mesa-Mt Taylor |
| 126901-5 | 587 | 256 | 488 | 17 | 81 | 132 | 215 | | Horace/La Jara Mesa-Mt Taylor |
| 126901-6 | 646 | 261 | 567 | 13 | 95 | 142 | 234 | | Horace/La Jara Mesa-Mt Taylor |
| 126901-7 | 589 | 226 | 501 | 17 | 82 | 134 | 208 | | Horace/La Jara Mesa-Mt Taylor |
| 126901-8 | 643 | 263 | 554 | 13 | 89 | 142 | 229 | | Horace/La Jara Mesa-Mt Taylor |
| 126902 | 466 | 77 | 120 | 47 | 19 | 108 | 55 | | Canovas Canyon Rhy |
| 126913 | 434 | 70 | 169 | 13 | 47 | 179 | 58 | | Valles Rhy (Cerro del Medio) |
| 126928 | 413 | 74 | 124 | 46 | 21 | 109 | 46 | | Canovas Canyon Rhy |
| 126938-1 | 482 | 696 | 157 | 19 | 41 | 125 | 42 | | Valles Rhy (Cerro del Medio) |
| 126938-2 | 655 | 265 | 516 | 18 | 87 | 151 | 226 | | Horace/La Jara Mesa-Mt Taylor |
| 127404-1 | 475 | 216 | 154 | 12 | 15 | 74 | 38 | | El Rechuelos Rhy |
| 127404-2 | 775 | 381 | 537 | 13 | 72 | 102 | 166 | | Grants Ridge-Mt Taylor |
| 127444 | 475 | 154 | 203 | 9 | 56 | 171 | 88 | | Cerro Toledo Rhy |
| 127453 | 581 | 230 | 532 | 12 | 92 | 141 | 217 | | Horace/La Jara Mesa-Mt Taylor |
| 127455 | 485 | 335 | 396 | 12 | 57 | 105 | 154 | | Grants Ridge-Mt Taylor |
| 127466 | 287 | 25 | -3 | 19 | 7 | 39 | 2 | | not obsidian |
| 127467 | 405 | 37 | 116 | 40 | 19 | 100 | 48 | | Canovas Canyon Rhy |

| Sample | Mn | Zn | Rb | Sr | Y | Zr | Nb | Ba | Source |
|----------|-----|-----|-----|-----|----|-----|-----|-----|----------------------------------|
| 127470 | 430 | 380 | 101 | 37 | 22 | 83 | 33 | 259 | Canovas Canyon Rhy |
| 127471 | 245 | 28 | 0 | 16 | 3 | 15 | 1 | | not obsidian |
| 127484 | 458 | 79 | 121 | 42 | 27 | 108 | 55 | | Canovas Canyon Rhy |
| 127485 | 473 | 101 | 133 | 50 | 26 | 105 | 52 | | Canovas Canyon Rhy |
| 127488-1 | 419 | 226 | 99 | 40 | 21 | 81 | 39 | 313 | Canovas Canyon Rhy |
| 127488-2 | 661 | 406 | 532 | 20 | 91 | 131 | 206 | | Horace/La Jara Mesa-Mt Taylor |
| 127492-1 | 560 | 201 | 187 | 13 | 41 | 172 | 55 | | Valles Rhy (Cerro del Medio) |
| 127492-2 | 453 | 195 | 179 | 15 | 44 | 160 | 49 | | Valles Rhy (Cerro del Medio) |
| 127492-3 | 340 | 456 | 114 | 12 | 28 | 97 | 30 | <1 | Canovas Canyon Rhy |
| 127494 | 571 | 100 | 145 | 50 | 23 | 105 | 53 | | Canovas Canyon Rhy |
| 127500-1 | 392 | 411 | 74 | 29 | 15 | 59 | 20 | | too small, probably Canovas Cnyn |
| 127500-2 | 591 | 222 | 132 | 45 | 24 | 102 | 41 | | Canovas Canyon Rhy |
| 127501-1 | 470 | 106 | 123 | 48 | 18 | 102 | 50 | | Canovas Canyon Rhy |
| 127501-2 | 545 | 271 | 115 | 45 | 21 | 88 | 41 | 261 | Canovas Canyon Rhy |
| 127501-3 | 560 | 127 | 125 | 48 | 21 | 113 | 46 | | Canovas Canyon Rhy |
| 127501-4 | 487 | 57 | 130 | 43 | 20 | 108 | 57 | | Canovas Canyon Rhy |
| 127501-5 | 469 | 74 | 123 | 44 | 26 | 107 | 46 | | Canovas Canyon Rhy |
| 127504 | 420 | 130 | 116 | 43 | 21 | 97 | 48 | | Canovas Canyon Rhy |
| 127508 | 571 | 226 | 136 | 47 | 17 | 105 | 49 | | Canovas Canyon Rhy |
| 127511 | 681 | 348 | 538 | 13 | 79 | 125 | 195 | | Grants Ridge-Mt Taylor |
| 127512 | 460 | 73 | 125 | 48 | 25 | 109 | 57 | | Canovas Canyon Rhy |
| 127514-1 | 464 | 100 | 123 | 47 | 21 | 107 | 50 | | Canovas Canyon Rhy |
| 127514-2 | 457 | 65 | 127 | 47 | 22 | 113 | 56 | | Canovas Canyon Rhy |
| 127516 | 467 | 182 | 114 | 47 | 24 | 103 | 46 | | Canovas Canyon Rhy |
| 127523 | 422 | 95 | 117 | 46 | 18 | 98 | 54 | | Canovas Canyon Rhy |
| 127528 | 634 | 458 | 125 | 45 | 19 | 85 | 43 | | Canovas Canyon Rhy |
| 127529 | 485 | 95 | 133 | 46 | 25 | 105 | 52 | | Canovas Canyon Rhy |
| 127531 | 576 | 245 | 575 | 12 | 95 | 140 | 226 | | Horace/La Jara Mesa-Mt Taylor |
| RGM1-S4 | 309 | 42 | 147 | 106 | 23 | 216 | 3 | 813 | standard |
| RGM1-S5 | 296 | 43 | 139 | 106 | 21 | 214 | 10 | | standard |
| RGM1-S4 | 316 | 45 | 141 | 111 | 19 | 214 | 9 | | standard |
| RGM1-S4 | 291 | 40 | 143 | 101 | 24 | 209 | 12 | | standard |

¹ Ba analyzed only when helpful in source assignment (see Davis et al. 2011).

Table 2. Frequency distribution of obsidian source provenance (non-obsidian and samples too small to assign not tabulated).

| | Frequency | Percent |
|--------------------------------|-----------|---------|
| MOUNT TAYLOR SOURCES | | |
| Horace/La Jara Mesa-Mt Taylor | 19 | 31.7 |
| Grants Ridge-Mt Taylor | 6 | 10.0 |
| JEMEZ MOUNTAINS SOURCES | | |
| Canovas Canyon Rhy | 29 | 48.3 |
| Valles Rhy (Cerro del Medio) | 4 | 6.7 |
| Cerro Toledo Rhy | 1 | 1.7 |
| El Rechuelos Rhy | 1 | 1.7 |
| Total | 60 | 100.0 |

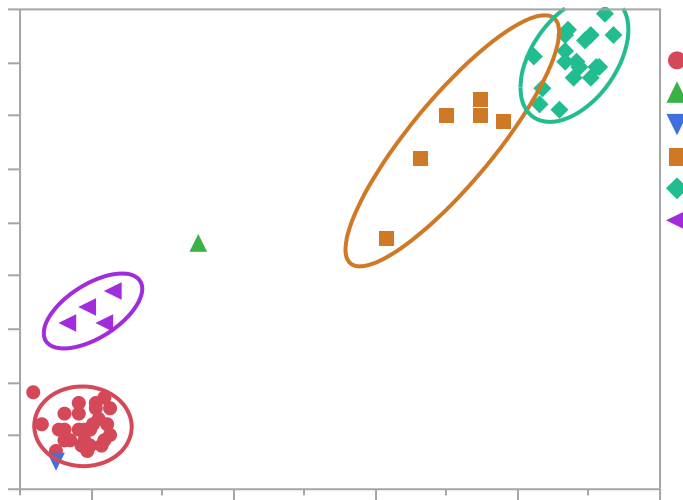


Figure 1. Nb versus Y bivariate plot of all artifacts. Ellipses are at 95% confidence intervals for individual sources.

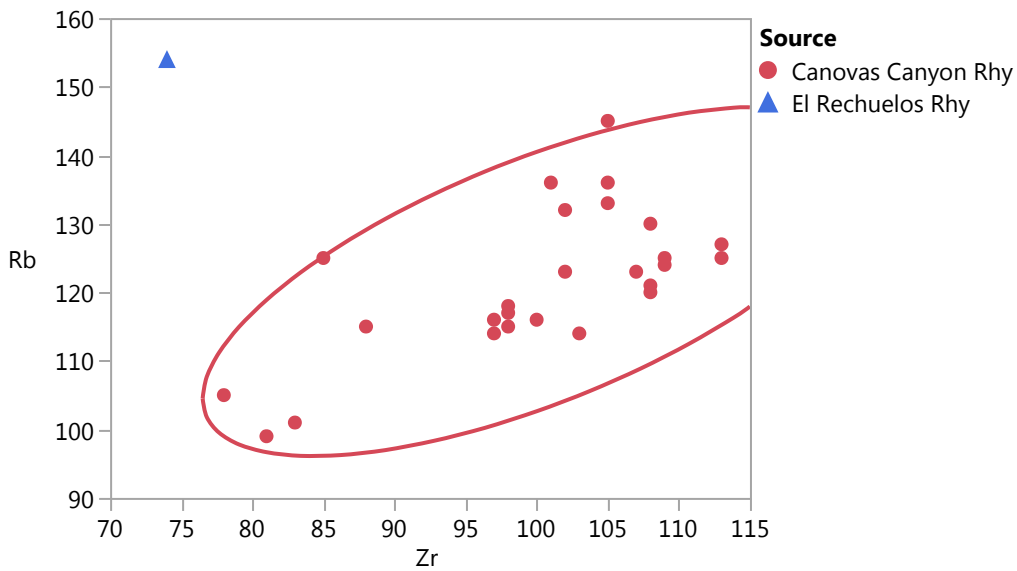


Figure 2. Zr versus Rb bivariate plot of the high Sr artifacts assigned as Canovas Canyon Rhyolite or El Rechuelos Rhyolite. Ellipse is at 95% confidence interval for individual sources.

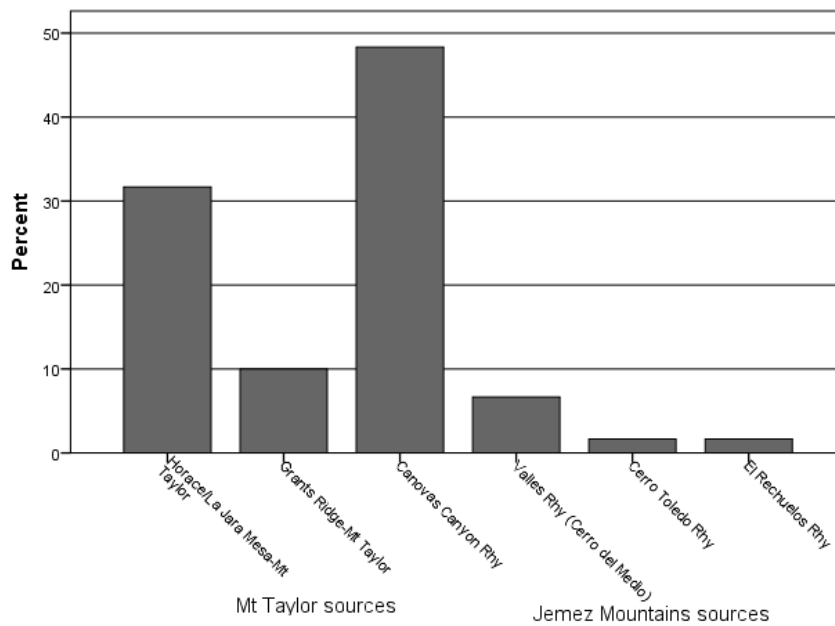


Figure 3. Frequency histogram of obsidian source provenance. See Table 2.

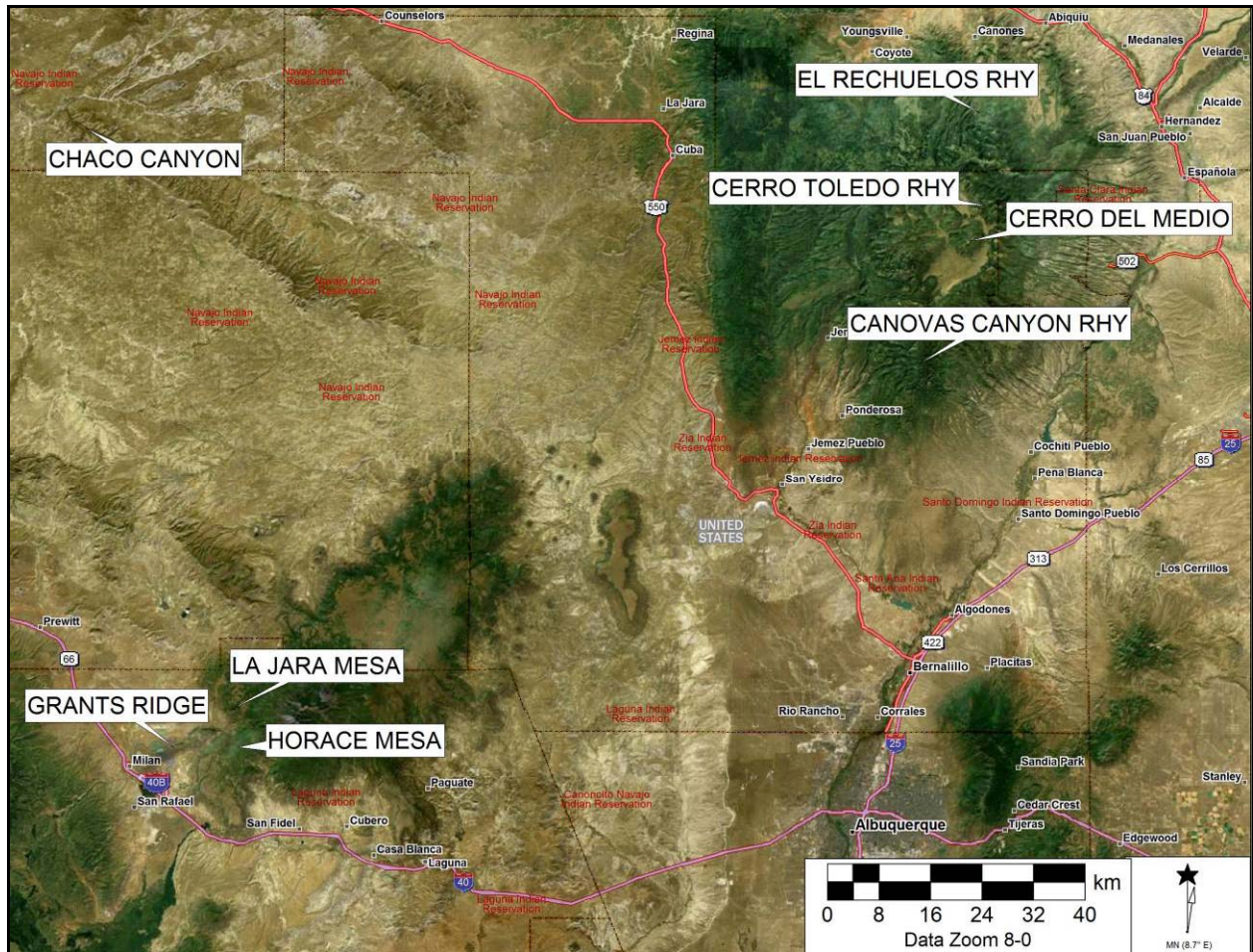


Figure 4. Satellite ortho-photo of Chaco Culture Historical Park and obsidian sources present in the assemblage.